Journal of Power Sources 196 (2011) 5077–5083

Contents lists available at ScienceDirect

Journal of Power Sources

journal homepage: www.elsevier.com/locate/jpowsour

Comparison of degradation behaviors for open-ended and closed proton exchange membrane fuel cells during startup and shutdown cycles

Yi Yu[a,b,*], Zhengkai Tu[a,b], Haining Zhang[a,b], Zhigang Zhan[a,b], Mu Pan[a,b]

[a] State Key Laboratory of Advanced Technology for Materials Synthesis and Processing, Wuhan University of Technology, Wuhan 430070, China
[b] Hubei Provincial Key Laboratory of Fuel Cell, Wuhan 430070, China

ARTICLE INFO

Article history:
Received 13 January 2011
Accepted 20 January 2011
Available online 28 January 2011

Keywords:
Proton-exchange membrane fuel cell
Startup and shutdown cycles
Performance decay
Carbon corrosion

ABSTRACT

As catalyst support materials, the oxidation of carbon materials is considered one of the major factors for performance decay during the startup and shutdown process of proton exchange membrane fuel cells, which must be mitigated to achieve acceptable durability. In this paper, the effect of cathode exhaust conditions on the degradation behaviors of fuel cells is investigated using two single cells named the open-ended and closed cells. The cathode inlet pressure during the introduction of the dummy load is an important factor in analyzing the performance decay of membrane electrode assemblies under different conditions. Electrochemical techniques, including the measurement of polarization curves, cyclic and linear sweep voltammetry, and cross-sectional scanning electron microscopy of tested membrane electrode assemblies, are employed to evaluate the performance decay of fuel cells. The results show that a closed cathode exhaust valve during the introduction of the dummy load would significantly alleviate both the performance decay and the decrease in the electrochemically active surface area, resulting in an improvement in fuel cell durability. No significant deterioration of the membranes is observed for both the open-ended and the closed cells during frequent startup and shutdown processes.

1. Introduction

The proton exchange membrane fuel cell (PEMFC) has been considered one of the most promising clean energy sources of the 21st century for transportation and stationary applications due to the high energy conversion efficiency and power density, fast startup time and low/zero emission level [1]. However, some technological "bottlenecks" for current PEMFC technology have limited its further commercialization. For example, the relatively short lifetime of PEMFCs induced by the degradation of the materials is still unsatisfactory for stationary and mobile applications [2,3].

For mobile applications, PEMFCs must be operated under various conditions, such as load changing cycles, high power conditions, idling conditions and startup and shutdown cycles. Pei et al. investigated the durability of PEMFCs and evaluated its lifetime under these different conditions [4]. The results suggested that performance decay under frequent startup and shutdown cycles was very serious. Consequently, it is essential to investigate the system strategies to enhance the durability of PEMFCs under startup and shutdown cycles [5]. In 2005, a new decay mechanism related to local hydrogen starvation, which possibly presented during startup and shutdown procedures, was described by United Technologies Corporation (UTC) [6]. They pointed out that air was present on both the anode and the cathode before the startup process of PEMFCs. When introducing hydrogen to the anode, hydrogen only occupied part of the electrode, resulting in an air/H_2 boundary at the anode and causing carbon corrosion and irreversible deterioration of the cell performance [7]. Tang et al. [8] investigated the effect of unprotected startup and shutdown on PEMFC performance degradation using both single cell and dual cell configurations. The cathode potential as high as two times the open circuit voltage was observed after shutdown or during its restart. Kim et al. [9] investigated the relationship between carbon corrosion and positive electrode potential in a fuel cell during start/stop operations. The positive electrode potential increased to 1.4 V when the air/hydrogen boundary was formed on the anode.

Recently, many research groups have paid more attention on the system strategies of startup and shutdown operations to enhance the durability of PEMFCs. The group of the Fuel Cell Research Center at the Korea Institute of Science and Technology has been developing several methods to improve the durability of PEMFCs [10–12]. Kim et al. [10] investigated the effects of applying a dummy load on the degradation of a single cell. Their results suggested that applying a dummy load in starting up PEMFCs was an effective way to mitigate performance degradation. Kim et al. [11] reported the effects of cathode inlet relative humidity on PEMFC durability during startup and shutdown cycling. The performance was better for PEMFCs cycled at a lower cathode inlet RH than for those cycled at

* Corresponding author: Tel.: +86 13277077841; fax: +86 27 87879468.
E-mail address: yuyiwhut08@gmail.com (Y. Yu).

0378-7753/$ – see front matter © 2011 Elsevier B.V. All rights reserved.
doi:10.1016/j.jpowsour.2011.01.075

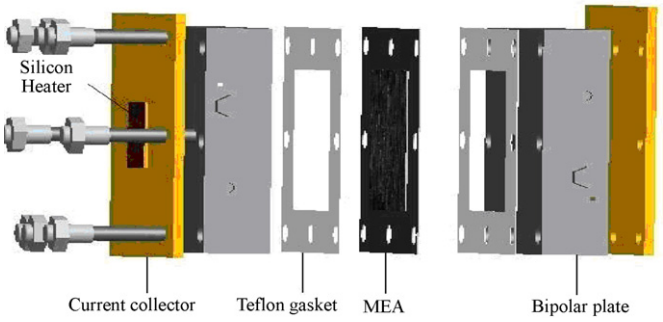

Fig. 1. Schematic diagram of single cells used in the experiment.

a higher cathode inlet RH on the order of 0 > 50 > 100%. Jo et al. [12] investigated the effects of hydrogen and the air supply sequence during the startup process on the durability of PEMFCs. These results suggest that supplying hydrogen prior to air can effectively mitigate performance degradation by retarding the degradation of the electrodes rather than the membrane.

However, some of the above methods cannot be realized in the automotive fuel cell engine. To simulate a real startup and shutdown process, we investigated two different conditions of the exhaust valve in the cathode, which could be controlled easily in the fuel cell engine. To reveal the effect of cathode exhaust conditions on the performance decay, open-ended and closed cells were developed and investigated under specific startup and shutdown cycles. Different electrochemical and physicochemical techniques were applied to characterize the performance decay of single cells.

2. Experimental

2.1. Single cell test

A single cell with an active area of 25 cm^2 was fabricated with a commercially available MEA (Membrane Electrode Assembly), Teflon gaskets and seven serpentine flow fields on both sides of the MEA. The MEA consisted of the polymer electrolyte membrane (Nafion211) in combination with platinum loadings of 0.4 mg cm^{-2} per electrode. The gas diffusion layers were made of Toray carbon paper. The bipolar plates were tightened with gold-coated plates that were used for current collection. The schematic diagram of a single cell is shown in Fig. 1. After assembly of the single cells, leak tests were performed by nitrogen, and the leakage flux was not more than 0.1 nlpm.

The schematic diagram of the testing system is shown in Fig. 2. The testing system could be programmed precisely to control various operational parameters, including the electronic load, gas flux or excessive coefficient, dew point temperature and cell temperature. Fuel and air were passed through a bubble humidifier under ambient pressure before introducing them into the cell for the supply of fully humidified gases. The cell temperature was held at 65 °C. The stoichiometry of the fuel and air was 1.5 and 2.5, respectively, during recording the polarization curves.

2.2. Open/closed operation in startup and shutdown cycles

Before the startup and shutdown cycles, all the MEAs were pre-activated using H_2/air (100% RH) with varying current for 8 hours, and the polarization curves were recorded to characterize the performance of fresh MEAs.

The startup and shutdown repetition (1500 cycles) was carried out with the following steps. Step 1, the single cells were set to the open-circuit voltage (OCV) state for 30 s. Fully hydrated hydrogen and air with a stoichiometry of 1.5 and 2.5, respectively, were fed to the anode and cathode. Step 2, the air supply was shut off with the introduction of a dummy load, which could eliminate the residual O_2 in the cathode gas channel. When the cell voltage was below 0.05 V, the hydrogen supply was stopped. In this process, the open-ended cell was kept as the cathode exhaust valve opened, whereas the closed cell was kept closed. The electrochemical processes in the two single cells are shown in Fig. 3. Finally, after 10 s of shutting off the hydrogen supply, the dummy load was removed. At the same time, hydrogen and air were fed into the cells. The change in current density for one cycle, as the time scale, is shown in Fig. 4.

After every 300 cycles, the performance of the single cells was characterized by polarization curves, cyclic voltammetry (CV) and linear sweep voltammetry (LSV). CV was implemented to determine the electrochemical active surface area (ECSA) of the Pt catalysts. For the CV method, the working electrode was flushed with nitrogen, and the other electrode was flushed with hydrogen, with the polymer membrane as the electrolyte. Using a potentiostat, the system potential was swept between two voltage limits while current was recorded, and a plot of the current vs. voltage was generated [13]. The applied potential was cycled from 0.05 to 1.2 V with a scan rate of 0.05 Vs^{-1}. Similarly, LSV was applied to determine the hydrogen crossover of the MEAs, applying potential in the range from 0.05 to 0.7 V at a scan rate of 2 mVs^{-1}.

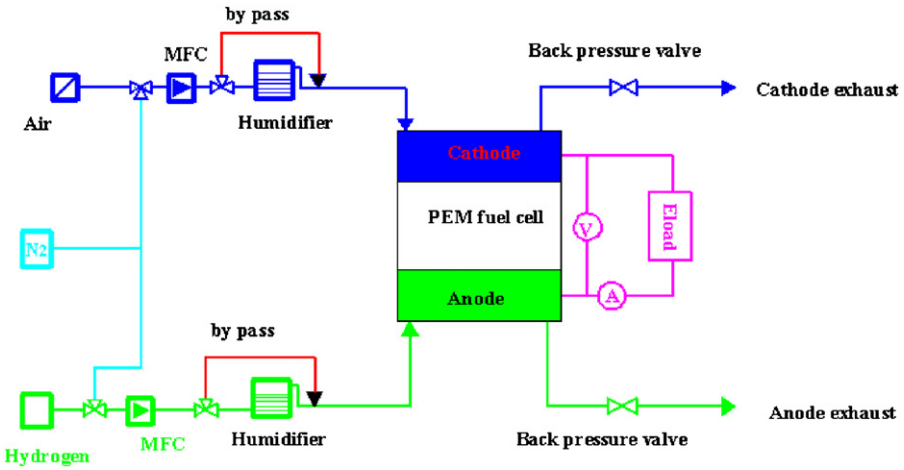

Fig. 2. The schematic diagram of the test system.

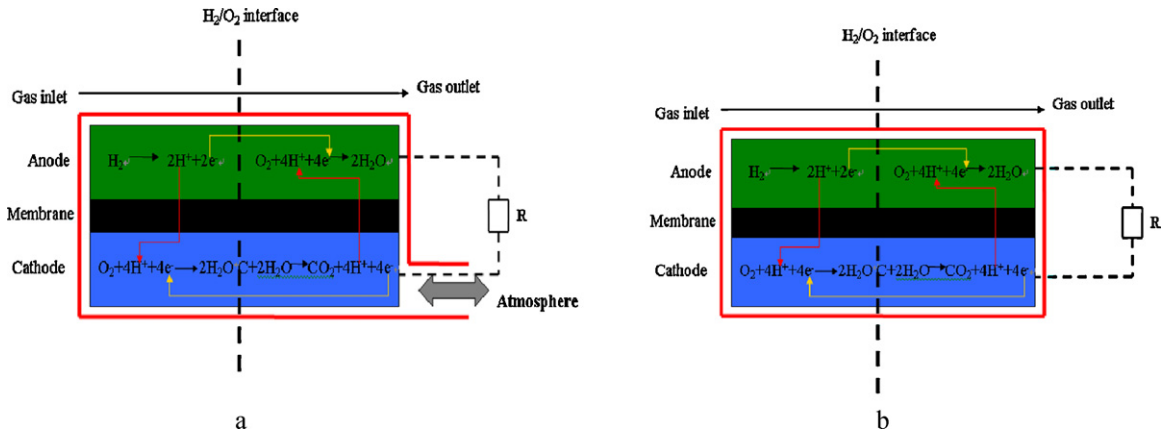

Fig. 3. The electrochemical process for (a) open-ended cell and (b) closed cell in the startup–shutdown cycles.

3. Result and discussion

3.1. Startup and shutdown operation

Fig. 5 shows the experimental load profiles and cathode inlet pressure change in one cycle for two cells: (a) for the open-ended cell and (b) for the closed cell. In step 2, when the air supply was shut off with the introduction of a dummy load, the voltage of both cells dropped to 0.8 V and decreased slowly for 40 s. However, the voltage dropped rapidly to nearly 0 V within the next 15 s. For the open-ended cell, the voltage dropped to approximately 0 V when the cathode inlet pressure was nearly 5 kPag (Fig. 5a), whereas the cell voltage dropped to 0 V for the closed cell until the cathode inlet pressure was nearly 0 kPag (Fig. 5b). When the cathode exhaust valve was open, the residual gas in the channel would flow outside the cell, which could lead to the pressure drop in the cathode channel. Under this pressure drop, the reaction gas in the inlet pipe would spread into the cell, such that the inlet pressure of the open-ended cell did not decrease to 0 kPag. Whereas, the gas equilibrium in the closed cell induced the inlet pressure to decrease to approximately 0 kPag.

In the cathode of both cells, the oxygen concentration decreased with the consumption under the electrochemical reaction after the introduction of the dummy load. When the cathode exhaust valve was open, air in the exhaust pipe would spread into the cell from the open end. This could lead to an imbalance of gas distribution in the plane direction of the flow field, resulting in the bias of oxygen pressure in the anode [14]. In this case, the H_2/O_2 interface existing in the cell lasts a relatively long period of time. According to the "reverse-current mechanism" [6], it is not beneficial to the durability of the carbon support in PEMFCs.

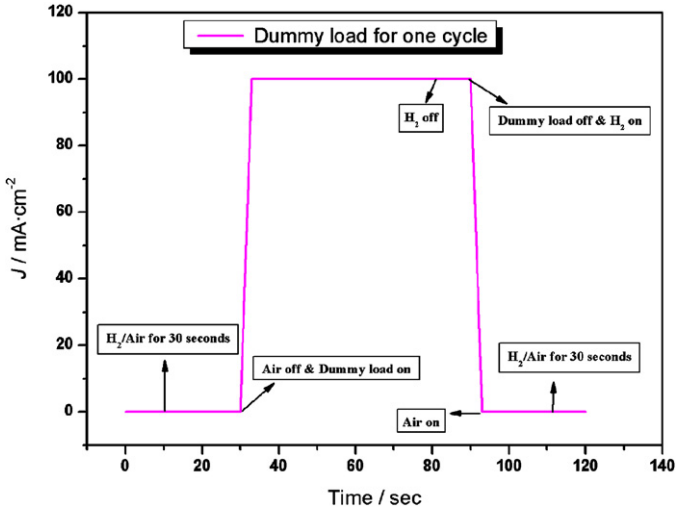

Fig. 4. Change of current density as a function of time in one cycle.

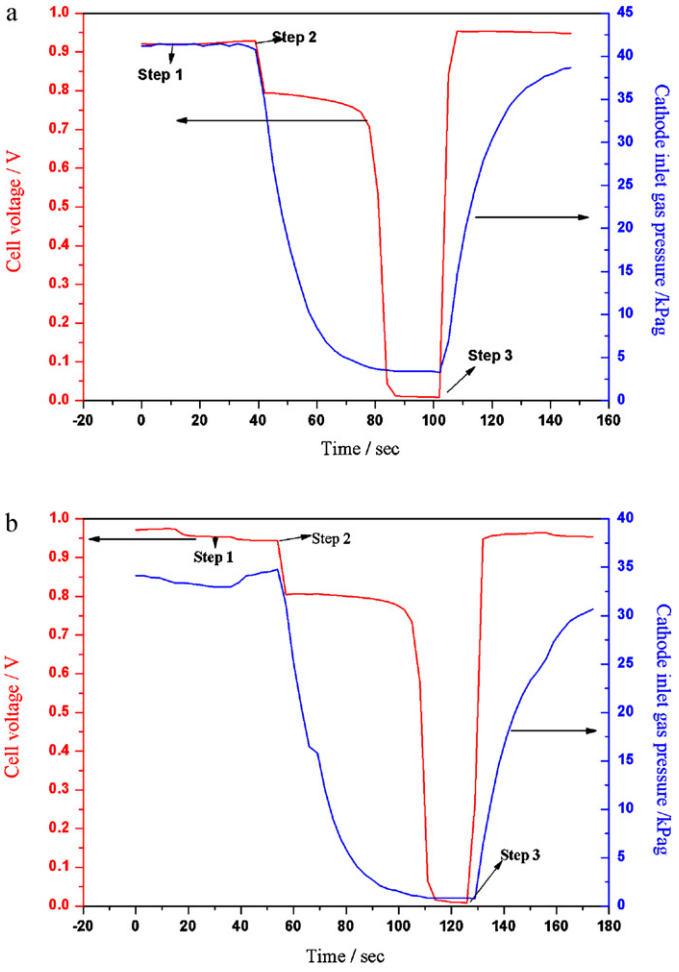

Fig. 5. Variation of cell voltage and cathode inlet pressure: (a) open-ended cell and (b) closed cell.

3.2. Polarization curves

Cell performance was evaluated by polarization curves. Fig. 6 shows the polarization curves of fresh MEA and after 300, 600, 900,

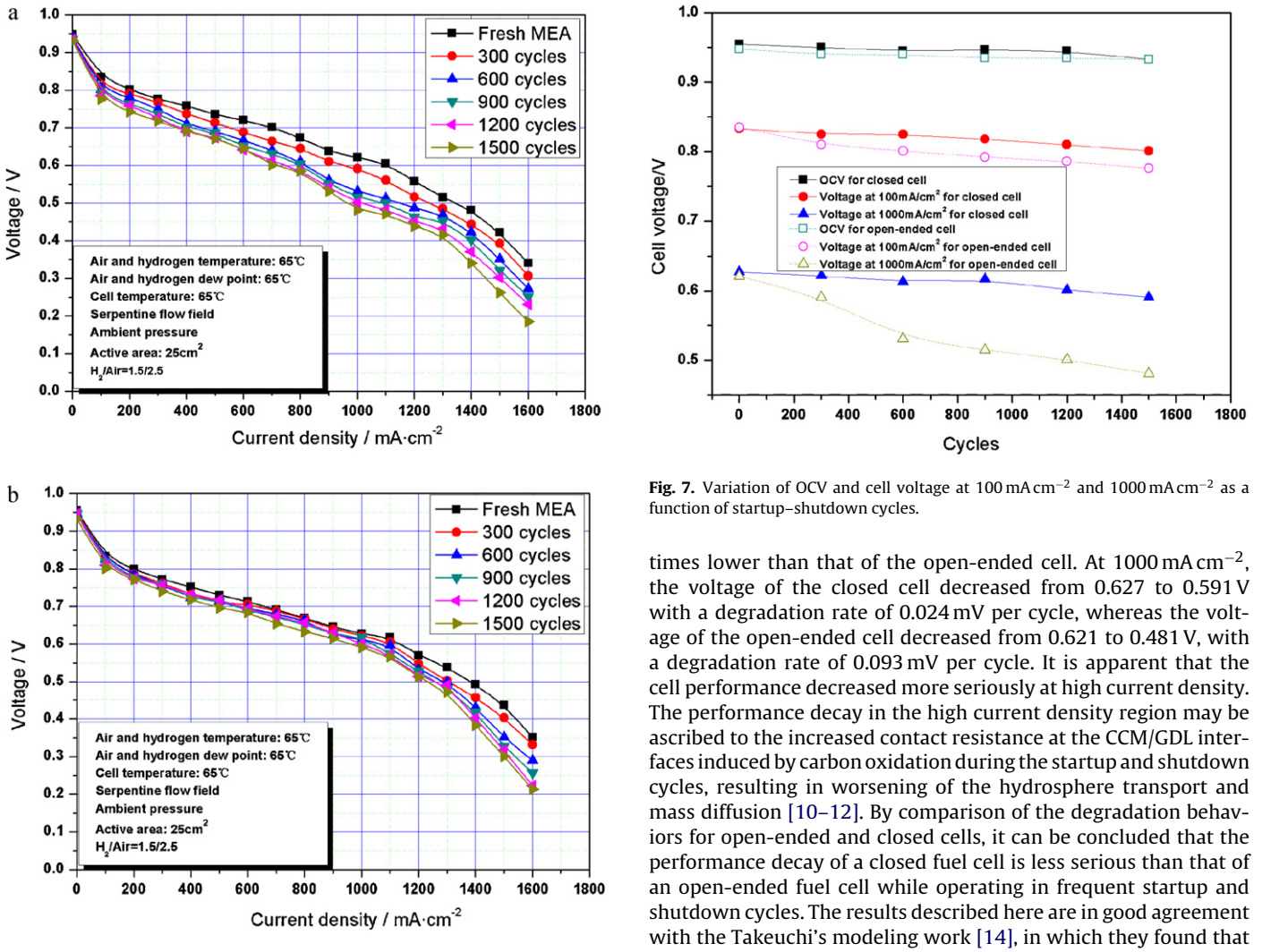

Fig. 6. Polarization curves of (a) open-ended cell and (b) closed cell during 1500 startup–shutdown cycles.

Fig. 7. Variation of OCV and cell voltage at 100 mA cm^{-2} and 1000 mA cm^{-2} as a function of startup–shutdown cycles.

1200 and 1500 startup and shutdown cycles for the open-ended cell (a) and the closed cell (b). It can be seen that the performance of both cells decreases with the increase in the number of operating cycles. However, the performance decay for the open-ended cell was more serious compared to that for the closed cell, especially after 1500 startup and shutdown cycles.

The performance degradation in different current density regions was characterized by the degradation rates of the cell voltage under certain current densities. According to St. Pierre [15,16], the degradation rate can be calculated by the following formula:

$$\text{Degradation rate (mV/cycle)} = \frac{\text{final performance (mV)} - \text{original performance (mV)}}{\text{cycle number}}$$

Fig. 7 shows the degradation of the OCV and voltage at 100 and 1000 mA cm^{-2} as a function of the startup and shutdown cycles. For both single cells, the value of the OCV only slightly decreased, indicating that the gas crossover through the MEA did not significantly increase and that the proton exchange membranes in both cells did not deteriorate. However, after 1500 cycles, the voltage of the open-ended cell at 100 mA cm^{-2} decreased from 0.835 to 0.776 V with a degradation rate of 0.0393 mV per cycle. In comparison, the voltage of the closed cell decreased from 0.833 to 0.801 V, and the degradation rate was 0.0213 mV per cycle, almost two times lower than that of the open-ended cell. At 1000 mA cm^{-2}, the voltage of the closed cell decreased from 0.627 to 0.591 V with a degradation rate of 0.024 mV per cycle, whereas the voltage of the open-ended cell decreased from 0.621 to 0.481 V, with a degradation rate of 0.093 mV per cycle. It is apparent that the cell performance decreased more seriously at high current density. The performance decay in the high current density region may be ascribed to the increased contact resistance at the CCM/GDL interfaces induced by carbon oxidation during the startup and shutdown cycles, resulting in worsening of the hydrosphere transport and mass diffusion [10–12]. By comparison of the degradation behaviors for open-ended and closed cells, it can be concluded that the performance decay of a closed fuel cell is less serious than that of an open-ended fuel cell while operating in frequent startup and shutdown cycles. The results described here are in good agreement with the Takeuchi's modeling work [14], in which they found that the open state of the exhaust valve increased the bias of oxygen pressure in the anode and the existing time of the H_2/O_2 interface, leading to severe performance degradation.

3.3. Electrochemical analyses

Cyclic and linear sweep voltammetry are important methods in evaluating the degradation of the MEA after frequent startup and shutdown cycles. The *in situ* CV technique has proven to be quite valuable for ascertaining the electrochemical surface area of the electrodes, as previously described [13,17–19]. Fig. 8 shows the cyclic voltammograms of open-ended and closed cells during 1500 startup and shutdown cycles. The hydrogen desorption peak decreased with an increase in the number of startup and shutdown cycles. It can be clearly seen that the degradation in the cathode (Fig. 8A and C) was more severe than that in the anode (Fig. 8B and D) after frequent cycles for both cells.

Nanoscale Pt particles are usually distributed on carbon support materials to obtain a maximum utilization ratio and to decrease the cost of fuel cells. However, under prolonged operation at high temperatures, high water content, high oxygen concentration, low pH, existence of the Pt catalyst and/or high potential, the carbon support is prone to degrade both physically and chemically, called carbon oxidation [20]. Carbon corrosion may occur as a chemical or an electrochemical process. In addition to local fuel starvations [21], both startup and shutdown processes can cause a high potential in the cathode of the fuel cell. Reiser et al. have explained the decay phenomenon with one-dimensional electrochemical poten-

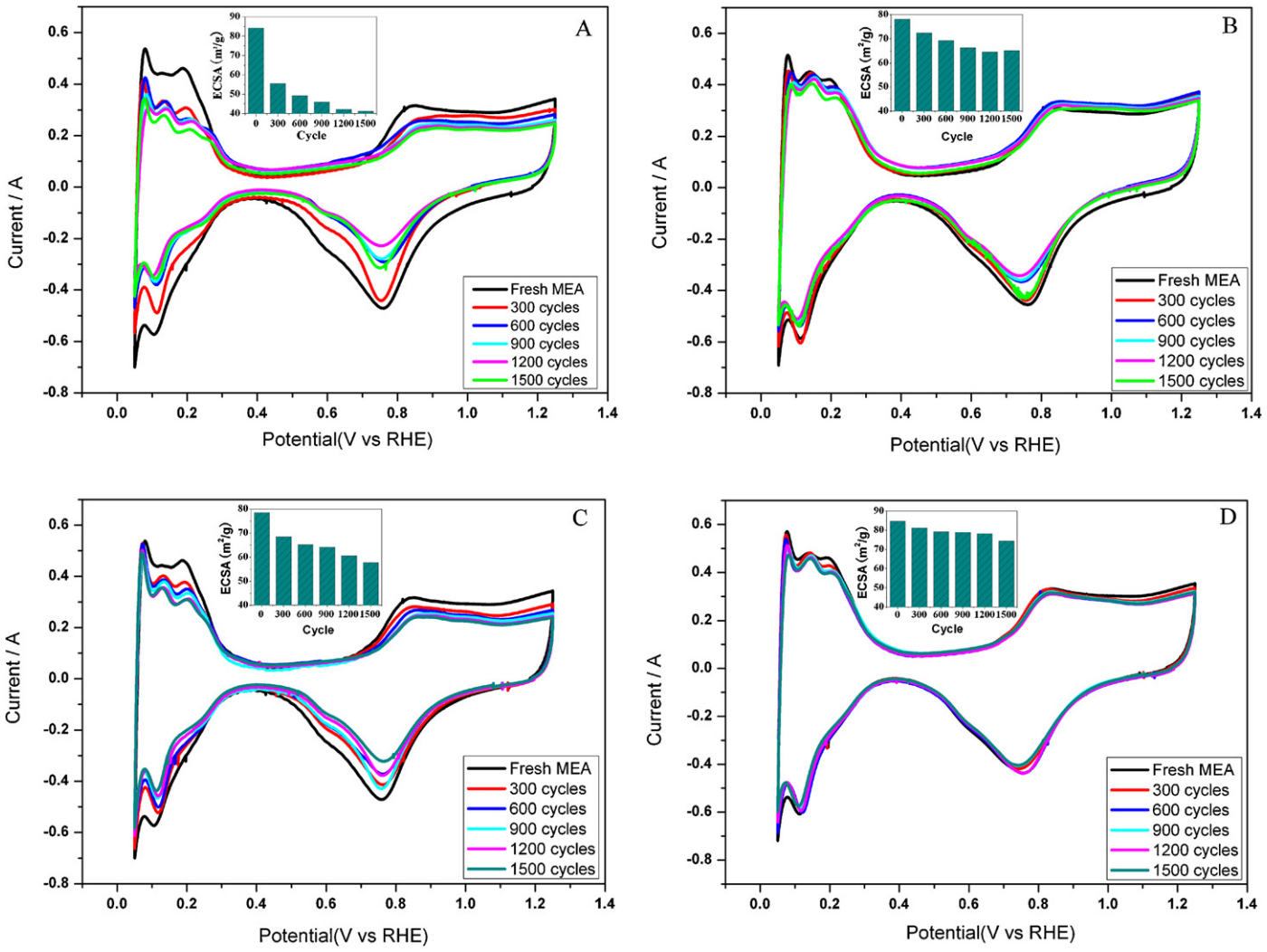

Fig. 8. Cyclic voltammograms during 1500 startup–shutdown cycles: (A) cathode of open-ended cell; (B) anode of open-ended cell; (C) cathode of closed cell; (D) anode of closed cell.

tial profile mode, using simplified mathematical approaches [6]. During the shutdown process of the PEMFC, the cathode interfacial potential difference was raised to 1.44 V. At such high potential, the carbon in the catalyst layer can be corroded within a few hours, damaging the cathode electrode, even for low-temperature polymer electrolyte fuel cells, according to the following reaction [21–23]:

$$C + 2H_2O \rightarrow CO_2 + 4H^+ + 4e^-, \quad E_{00} = 0.207\,V \tag{1}$$

$$C + H_2O \rightarrow CO + 2H^+ + 2e^-, \quad E_{00} = 0.518\,V \tag{2}$$

Carbon oxidation weakens the attachment of Pt particles to the carbon surface and eventually leads to structural collapse and detachment from the carbon support, leading to the agglomerate and/or the dissolving of Pt particles into the electrolyte without redeposition. Nanoparticles have the inherent tendency to agglomerate into bigger particles to reduce the high surface energy [21,24]. Moreover, Pt may be transported through the electrolyte and/or through the ionomer [25]. Therefore, the carbon oxidation, which was caused by the high potential, is the main reason for the catalyst degradation occurring in the cathode of the fuel cell.

However, for the catalyst layer in the anode, the interfacial potential difference was kept at the open-circuit voltage during the startup and shutdown process. At this potential, the oxidation of carbon in the anode was much slower than that in the cathode,

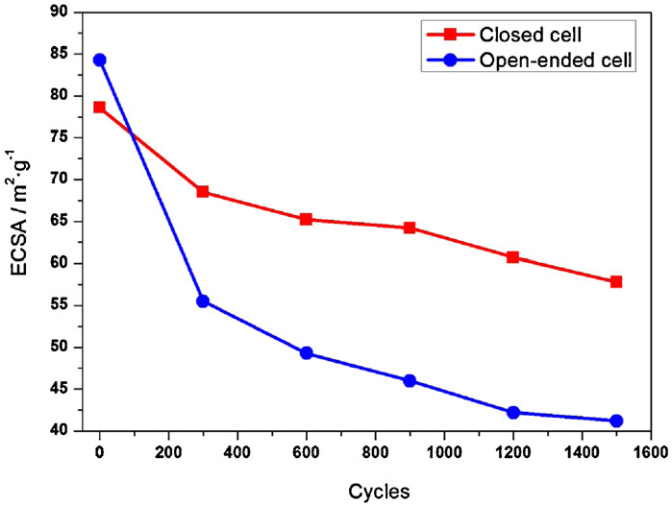

Fig. 9. Cathode ECSA for open-ended cell (circles) and closed cell (squares) during 1500 startup–shutdown cycles.

according to the kinetics of the electrochemical reaction. Therefore, the degradation rate of the catalyst layer in the anode is less pronounced than in the cathode, as shown in the cyclic voltammograms.

As shown in Fig. 8(A–D), the decay of the catalyst layer in the open-ended cell was more serious than that in the closed cell, especially at the cathode. The electrochemical surface area (ECSA) was applied to evaluate the degradation of the MEA, which can be calculated by the following equation:

$$\mathrm{ECSA} = \frac{Q_H}{[\mathrm{Pt}] \times 0.21}$$

where [Pt] represents the amount of Pt catalyst per unit area of the electrode (mg cm^{-2}), Q_H is the charge area of the hydrogen desorption (mC cm^{-2}), and 0.21 mC cm^{-2} denotes the charge required to oxidize the hydrogen monolayer on bright Pt [10,26]. The data of the cathode ECSA for the open-ended cell and the closed cell are shown in Fig. 9. After 1500 cycles, the ECSA of the closed cell decreased from 78.6 to 57.8 m^2 g^{-1}. In contrast, the ECSA of the open-ended cell decreased more significantly from 84.3 to 41.2 m^2 g^{-1}. The loss ratio of the ECSA for the open-ended cell was approximately twice that for the closed cell, as can be seen from Table 1.

Table 1
Comparison of ECSA loss ratio between open-ended cell and closed cell.

ECSA	Single cell	
	Open-ended cell	Closed cell
0 cycle-ECSA (m^2 g^{-1})	84.3	78.6
1500 cycles-ECSA (m^2 g^{-1})	41.2	57.8
Loss ratio of ECSA	51.13%	26.46%

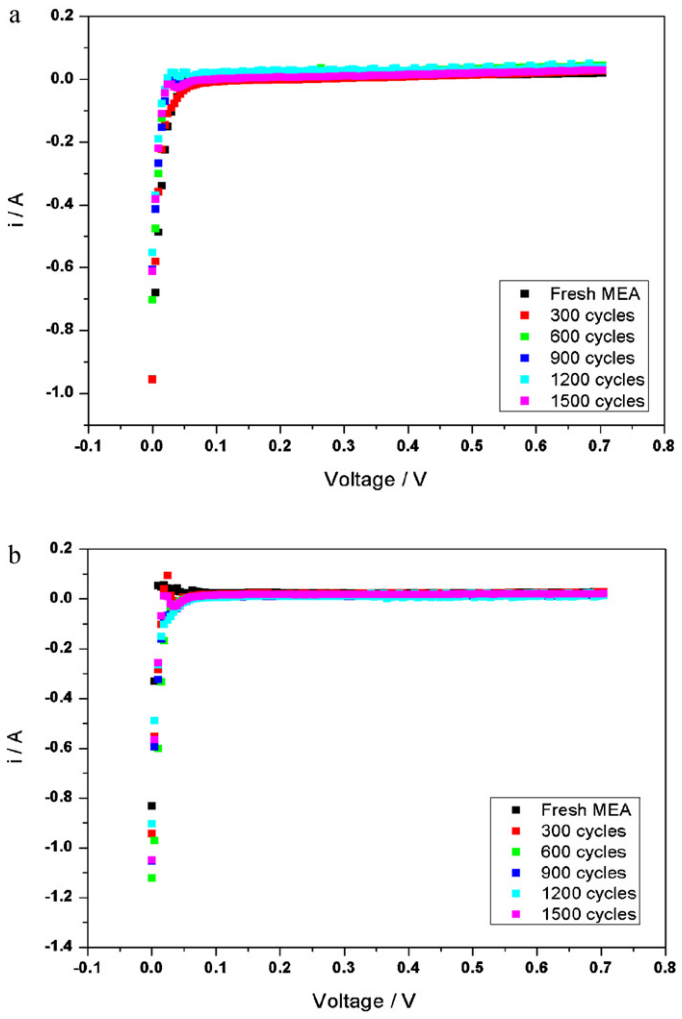

Fig. 10. Linear sweep voltammograms of MEAs in (a) open-ended cell and (b) closed cell during 1500 startup–shutdown cycles.

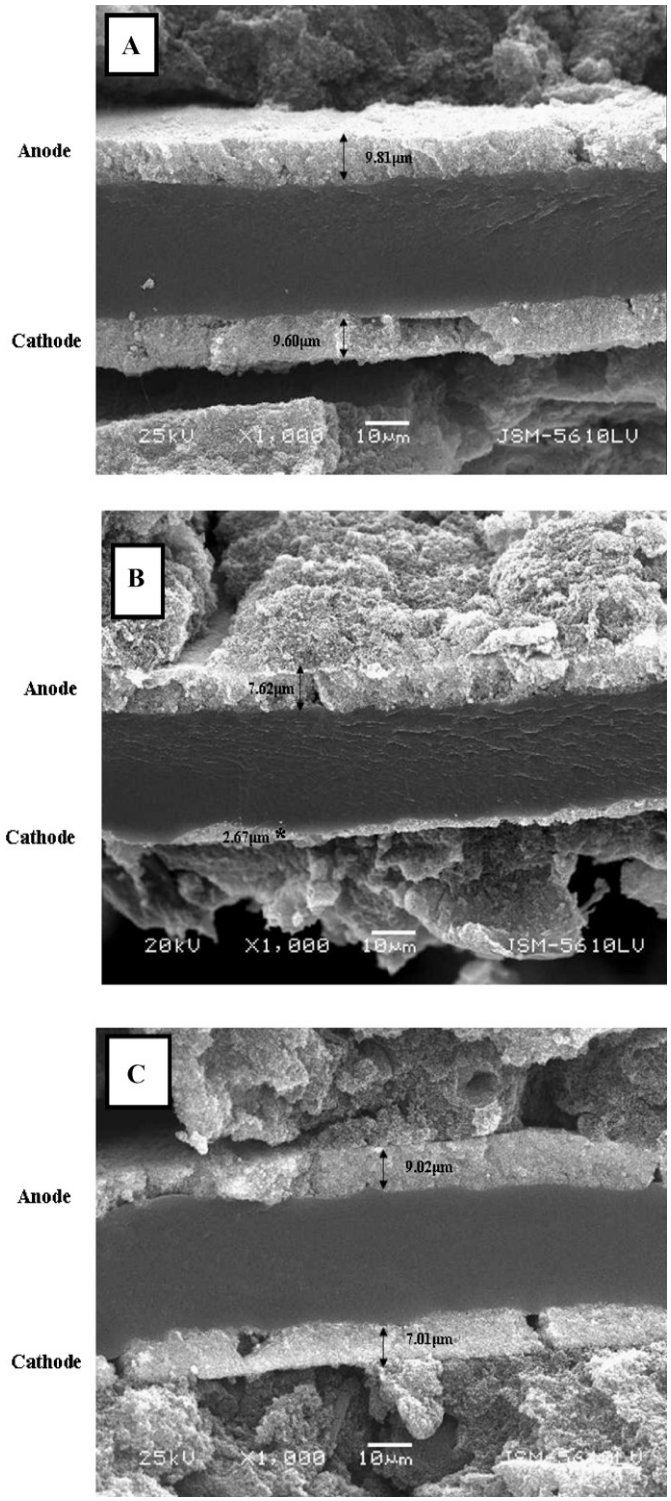

Fig. 11. Cross-sectional SEM images: (A) fresh MEA without startup–shutdown cycles; (B) MEA in open-ended cell after 1500 cycles; (C) MEA in closed cell after 1500 cycles.

Crossover of hydrogen through the membrane is considered to be one of the most important phenomena in PEMFCs, which leads to

decreased efficiency of the fuels [27]. The hydrogen crossover current and hydrogen permeability of the proton exchange membrane were measured by linear sweep voltammetry [28,29]. LSV curves of the fresh membrane and after every 300 cycles are shown in Fig. 10. The hydrogen crossover current density at 0.6 V was selected to evaluate the degree of gas permeability. By dividing the current by active area, the hydrogen current density of all the MEAs was constant before and after frequent startup and shutdown cycles, nearly 1 mA cm^{-2}. The result indicates that membranes in both the closed cell and the open-ended cell did not deteriorate significantly, which could also be confirmed from the variation in the OCV. Thus, the performance degradation in the single cells was mainly caused by the decay of the catalyst layer and was independent of the proton-exchange membrane.

3.4. Cross-sectional SEM of MEAs

At the end of the test of the two single cells, the MEAs were analyzed by cross-sectional scanning electron microscopy (SEM). As shown in Fig. 11, the SEM images of the MEAs before and after 1500 startup and shutdown cycles in both the open-ended cell and the closed cell were compared by the thickness of the electrolyte layers. The boundary among the membrane, catalyst and gas diffusion layer was significantly delaminated.

In Fig. 11A, the thickness of the catalyst layers in the anode and cathode of fresh MEAs was 9.81 and 9.60 μm, respectively. After 1500 cycles in the closed cell, the thickness of the catalyst layers had a slight change at the anode. At the cathode of the closed cell, the thickness decreased to 7.01 μm, as can be seen in Fig. 11C. However, Fig. 11B shows that the thickness of the catalyst layer at both the anode and the cathode in the open-ended cell was 7.02 and 2.47 μm, respectively. The degradation of the catalyst layer in the open-ended cell was more severe than that in the closed cell. Thus, closing the exhaust valve of the PEMFC while operating in frequent startup and shutdown cycles was an effective way to alleviate the degradation of the catalyst layer.

4. Conclusions

Two different conditions of cathode exhaust (open or closed) in frequent startup and shutdown cycles were investigated in open-ended and closed cells, respectively. The degradation behaviors of two single cells were analyzed and compared by various electrochemical and physicochemical techniques. Combined with the results of polarization curves, CV, LSV and cross-sectional SEM, the following conclusions can be drawn:

When the PEMFC was operated with frequent startup and shutdown cycles, a closed cell would significantly reduce the performance decay and the decrease in the electrochemically active surface area. In an open-ended cell, cell performance decreased significantly, especially at high current density. Therefore, a closed cell is much more durable than an open-ended cell during startup and shutdown processes.

The stability of the catalyst in frequent startup and shutdown cycles is important for the durability of PEMFCs. The performance decay is mainly due to the loss of active area in the catalyst. The catalyst in the cathode was more prone to oxidation than in the anode. The loss ratio of the ECSA for the open-ended cell was approximately twice that for the closed cell, which also could be found from the variation in the thickness of the catalyst layers in the cathode.

However, the membrane deteriorated neither in the open-ended cell nor in the closed cell, which was confirmed from the variation in the hydrogen crossover current and open-circuit voltage.

Acknowledgements

This work was financially supported by the Ministry of Science and Technology 863 Hi-Technology Research and Development Program of China (Grant Nos. 2008AA11A106 and 2008AA040503), the National Natural Science Foundation of China (Grant No. 50632050) and China Postdoctoral Science Foundation (Grant No. 20100471165).

References

[1] D.P. Wilkinson, J. St-Pierre, in: W. Vielstich, A. Lamm, H.A. Gasteiger (Eds.), Handbook of Fuel Cells—Fundamentals Technology and Applications, vol. 3, John Wiley & Sons, 2003, pp. 611–626.
[2] J. Wu, X. Yuan, J.J. Martin, H. Wang, J. Zhang, J. Shen, S. Wu, W. Merida, J. Power Sources 184 (2008) 104–119.
[3] N. Yousfi-Steiner, Ph. Mocoteguy, D. Candusso, D. Hissel, J. Power Sources 194 (2009) 130–145.
[4] P. Pei, Q. Chang, T. Tang, Int. J. Hydrogen Energy 33 (2008) 3829–3836.
[5] M.L. Perry, T.W. Patterson, C. Reiser, ECS Trans. 3 (2006) 783–795.
[6] C.R. Reiser, L. Bregoli, T.W. Patterson, J.S. Yi, J.D. Yang, M.L. Perry, T.D. Jarvi, Electrochem. Solid-State Lett. 8 (2005) A273–A276.
[7] K.H. Kangasniemi, D.A. Condit, T.D. Jarvl, J. Electrochem. Soc. 151 (2004) E125–E132.
[8] H. Tang, Z. Qi, M. Ramani, J.F. Elter, J. Power Sources 158 (2006) 1306–1312.
[9] J. Kim, J. Lee, Y. Tak, J. Power Sources 192 (2009) 674–678.
[10] J.H. Kim, E.A. Cho, J.H. Jang, H.J. Kim, T.-H. Lim, I.-H. Oh, J.J. Ko, S.C. Oh, J. Electrochem. Soc. 156 (2009) B955–B961.
[11] J.H. Kim, E.A. Cho, J.H. Jang, H.J. Kim, T.H. Lim, I.H. Oh, J.J. Ko, S.C. Oh, J. Electrochem. Soc. 157 (2010) B104–B112.
[12] Y.Y. Jo, E.A. Cho, J.H. Kim, T.-H. Lim, I.-H. Oh, J.H. Jang, H.-J. Kim, Int. J. Hydrogen Energy (2010) 1–7.
[13] J. Wu, X. Yuan, H. Wang, M. Blanco, J.J. Martin, J. Zhang, Int. J. Hydrogen Energy 33 (2008) 1735–1746.
[14] N. Takeuchi, T.F. Fuller, Abstract 116 Electrochem. Soc. 215th Meeting, San Francisco, CA, 2009.
[15] J. St-Pierre, J. Roberts, K. Colbow, S. Campbell, A. Nelson, J. New Mater. Electrochem. Syst. 8 (2005) 163–176.
[16] M. Luo, C. Huang, W. Liu, Z. Luo, M. Pan, Int. J. Hydrogen Energy 35 (2010) 2986–2993.
[17] S. Srinivasan, E.A. Ticianelli, C.R. Derouin, A. Redondo, J. Power Sources 22 (1988) 359–375.
[18] M. Wang, K. Woo, T. Lou, Y. Zhai, D.-K. Kim, Int. J. Hydrogen Energy 30 (2005) 381–384.
[19] G. Tamizhmani, G.A. Capuano, J. Electrochem. Soc. 141 (1994) 968–975.
[20] S. Zhang, X.-z. Yuan, J.N.C. Hin, H. Wang, K.A. Friedrich, M. Schulze, J Power Sources 194 (2009) 588–600.
[21] T.R. Ralph, S. Hudson, D.P. Wilkinson, ECS Trans. 1 (2006) 67–84.
[22] S. Maass, F. Finsterwalder, G. Frank, R. Hartmann, C. Merten, J. Power Sources 176 (2008) 444–451.
[23] Y. Sato, Z. Wang, Y. Takagi, ECS Trans. 3 (2006) 827–833.
[24] P.J. Ferreira, G.J. la O', Y. Shao-Horn, D. Morgan, R. Makharia, S. Kocha, H.A. Gasteiger, J. Electrochem. Soc. 152 (2005) A2256–A2271.
[25] A.V. Virkar, Y. Zhou, J. Electrochem. Soc. 154 (2007) B540–B547.
[26] A. Pozio, M. De Francesco, A. Cemmi, F. Cardellini, L. Giorgi, J. Power Sources 105 (2002) 13–19.
[27] S.S. Kocha, J.D. Yang, J.S. Yi, AICHE J. 52 (2006) 1916–1925.
[28] J. Wu, X. Yuan, J.J. Martin, H. Wang, D. Yang, J. Qiao, J. Ma, J. Power Sources 195 (2010) 1171–1176.
[29] M. Miller, A. Bazylak, J. Power Sources 196 (2011) 601–613.